The film thickness effect on the physical properties of NiO thin films elaborated by Sol-gel method

Said Benramache[1*], Yacine Aoun[2], Ali Arif[3]

[1]Material Sciences Department, Faculty of Sciences,
 Biskra University, 07000 Biskra, ALGERIA

[2]Mechanical Department,
 El-Oued University, 39000, El-Oued, ALGERIA

[3]Electrical Department, Faculty of Technology
 Biskra University, 07000 Biskra, ALGERIA

*Corresponding Author

Abstract: In this work, nickel oxide (NiO) was elaborated on glass substrate at by sol-gel technique. The NiO thin films were prepared with 0.8 M $Ni(NO_3)_2\,6H_2O$ annealed at 600°C for 2 h. The coating process was repeated for 13, 14, 15, 16 and 17 times to obtain a thin film, which corresponded to 124, 137, 143, 147 and 166 nm of film thickness. NiO thin films were observed as nanocrystalline with cubic structure at 166 nm with (111) and (200) peaks were observed. All NiO thin films have an average transmittance of about 80% in the visible region. The NiO thin films have a variety in the band gap energy from 3.87 to 3.94 eV. Because of the effect of deposition times, the minimum value was found at 166 nm where this condition has the highest Urbach energy. The NiO thin films have an electrical conductivity which was increased from 7.94×10^{-3} to 84×10^{-3} $(\Omega.cm)^{-1}$ when film thickness increases from 124 to 137 nm. In the end, the electrical measurements were investigated by the four-point method, with the results show good electrical conductivity at 166 nm.

Keywords: Nickel oxide, thin films, transparency, sol-gel method.

1. Introduction

Recently, semiconductors as oxides metallics are essential compounds for the development of ultra-high frequency components, gas sensors, photocatalyst, optoelectronics, lithium ion microbatteries, enamels, and cathode materials for alkaline batteries. Among these, nickel oxide (NiO) is a semitransparent p-type semiconductor material with a large direct band gap. This material also has a wide range of applications such as gas sensors, photocatalyst, dye-sensitized solar cells, electrochromic coatings, ultraviolet (UV) photo-detector, light weight structural components in aerospace, in ceramic structures, counter electrodes and anode layer of solid, as well as counter electrodes oxide fuel cells [1,2].

Nickel oxide NiO is a part of the transparent conductive oxides (TCO) family. It has potential applications for gas sensors because of its wide band gap (3.6-4.0 eV), and solar cells application due to the p-type semiconducting property. Its application as transparent diodes, transparent transistors, displays and defrosting windows is due to its transparency, and it can also be used for the UV photodetectors and touch screens due to its good responsivity [3–6].

Nanocrystalline NiO thin films can be produced by several techniques such as reactive evaporation, molecular beam epitaxy (MBE), magnetron sputtering technique, pulsed laser deposition (PLD), spray pyrolysis, sol–gel process, chemical vapor deposition, and electrochemical deposition [7–9]. NiO has been intensively studied as a promising material for gas sensors because of its wide band gap (3.6–4.0 eV) and high stability that are similar to ZnO [10,11].

Sol-gel spin coating method has been successfully employed for the deposition of nickel oxide (NiO) thin films on microscope glass substrate. The films were prepared with different layers from 13 to 17 layers. The aim of this tutorial work is to present some information of TCOs films, and then we will provide a detailed description on the optical and electrical properties of NiO. The films were deposited with different film layers then annealed at 600°C for 2 h in air.

2. Experimental

NiO solution were prepared by dissolving 0.8 M nickel nitrate hexahydrate ($Ni(NO_3)_2.6H_2O$). It was used as the starting material source in the solvent containing equal volumes of absolute H_2O, then drops of HCl was added as a stabilizer. The mixture solution was stirred and heated at 25–50°C for 3 h to yield a clear and transparent solution. The coating was made one day after the precursor was prepared. On the other hand, the direct calcination of $Ni(NO_3)_2\ 6H_2O$ follows the reaction as:

$$2Ni(NO_3)_2 6H_2O = 2Ni + 4NiO_2 + O_2 + 12H_2O \quad (1)$$
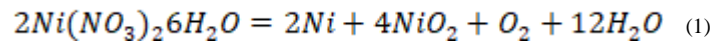
According to the above reaction, the NiO was the direct product of the calcinations, as the melting point of NiO is considerably high. In this work we will study the effect of thickness films on structural and optical properties of NiO thin films. The structural properties of the films were studied by means of X-ray diffraction (XRD; Bruker AXS-8D) with CuKα radiation (λ = 0.15406 nm) in the scanning range of 2θ between 30° and 50°. The optical transmittance of the deposited films was measured in the range of 300–1100 nm by using an ultraviolet-visible spectrophotometer (UV-Vis; LAMBDA 25) and the resistance, R was measured in a coplanar structure obtained with evaporation of four golden stripes on the deposited film surface. The measurements were performed with Keithley Model 2400 Low Voltage Source Meter instrument.

3. Results and Discussion

We report the XRD spectra of NiO at different film thickness as shown in Fig. 1. The XRD spectra of the samples revealed that the structure of NiO thin films is cubic structure ((JCPDS) No. 73- 1519) [12]. There were three diffraction peaks detected in the of XRD spectra, which are (101), (111) and (200) which are related to NiO phase. However, the (100) peak located at 2θ = 31° indicated the present of $Ni(OH)_2$ phase due to the smaller film thickness obtained. As the film thickness increased, the intensities of (111) and (200) peaks was enhanced, with the optimum result can be observed at 166 nm.
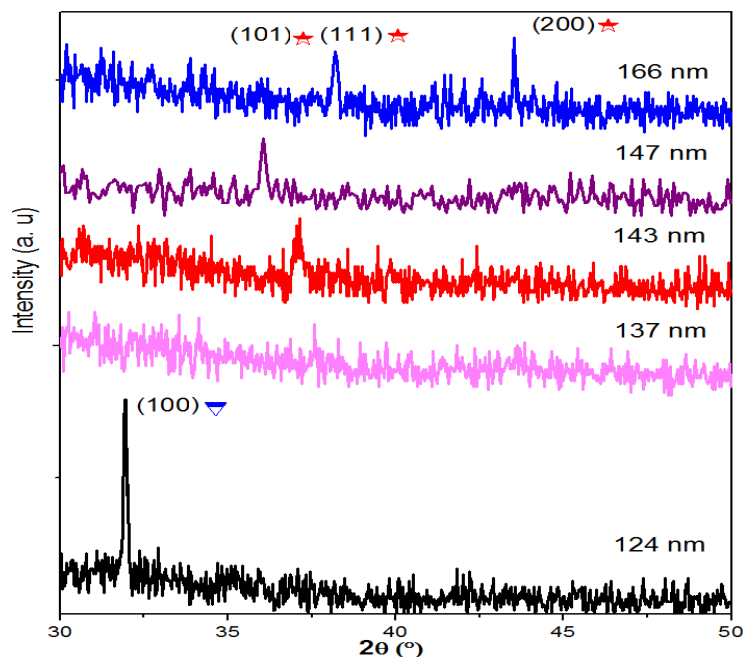

Fig. 1 - XRD patterns of NiO thin films prepared by sol-gel at different films thickness.

In order to calculate the crystallite size, G, of (111) and (200) diffraction peaks in NiO thin films prepared at 166 nm, we used Scherer's equation [13]:

$$G = \frac{0.9\lambda}{\beta \cos\theta} \qquad (2)$$

where λ = 1.5418 A°, β is the full width at half-maximum (FWHM), and θ is angle of diffraction peak. The values of crystallite sizes and FWHM are illustrated in Table 1. Note that the film prepared at 166 nm is nanostructure with cubic structure and the crystalline structure was improved at 166 nm.

Table 1 - The crystallite sizes and FWHM of NiO thin film prepared at 166 nm of (111) and (200) diffraction.

Diffraction peaks	2θ (°)	β (deg)	α (nm)	G (nm)
(111)	37.98	0.06	0.41032	24.43
(200)	43.53	0.04	0.4158	37.32

The optical transmission spectrum of NiO thin films with different film thickness is shown in Fig. 2. As seen, the NiO thin films have a high transparency of about 80% in the visible range. A very weak transmittance in the UV region which is close to 0% was also observed for all films. The region of strong absorbance for all films was observed between λ = 300 to 350 nm due to the excitation and the migration of the electrons from the valence band to the conduction band. It is clear that the films exhibit high transparencies in the visible spectral regions. Transmittance spectrum of NiO thin films indicates that the transmittance decreases as film thickness increases.
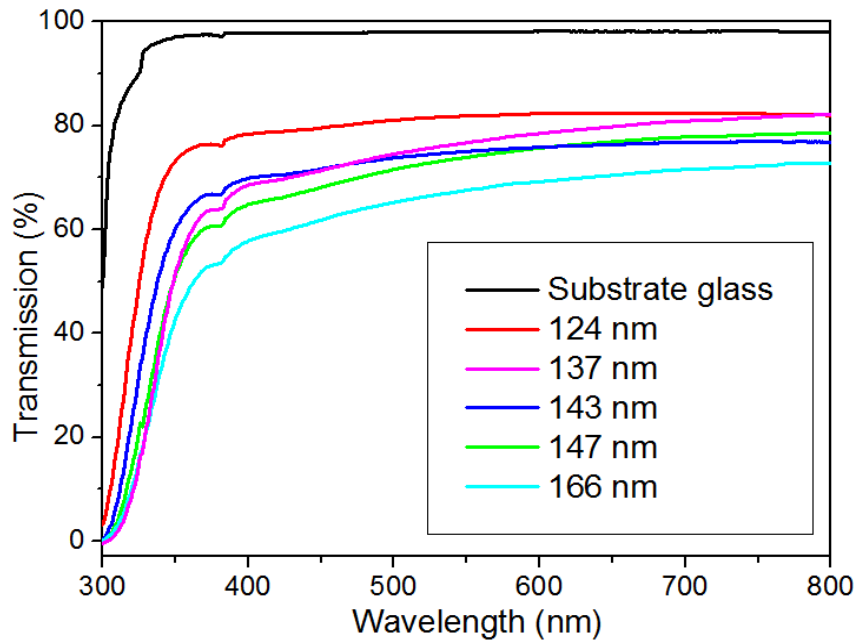
Fig. 2 - Optical transmittance spectra of NiO thin films as a function of film thickness.

The optical band gap, E_g was obtained by extrapolating the linear portion of the plot $(Ah\nu)^2$ versus $(h\nu)$ to $A = 0$ [23]. The graph in Fig. 3 was plotted according to the following equation [14]:

$$(Ah\nu)^2 = C(h\nu - E_g) \qquad (3)$$

where A is the absorbance, d is the film thickness; T is the transmission spectra of thin films; α is the absorption coefficient values; C is a constant, $h\nu$ is the photon energy, and E_g is the band gap energy of the semiconductor.

One can estimate the optical band gap (E_g) starting from the extrapolation of the curve which presents the evolution of $(Ah\nu)^2$ as a function of $h\nu$. The intersection of the linear region on the $h\nu$ axis gives the E_g. As shown in Fig. 3 and Table 2, there are variations of the band gap energy of the NiO thin films which were located around 3.96 eV. This is in good agreement with the E_g value of bulk NiO (3.6-4 eV) due to the p-type semiconductor [15]. But the film prepared at 166 nm have a minimum value is 3.87 eV which may be attributed to the improvement in the crystalline quality of the films, as well as to the increased in the crystallite size.
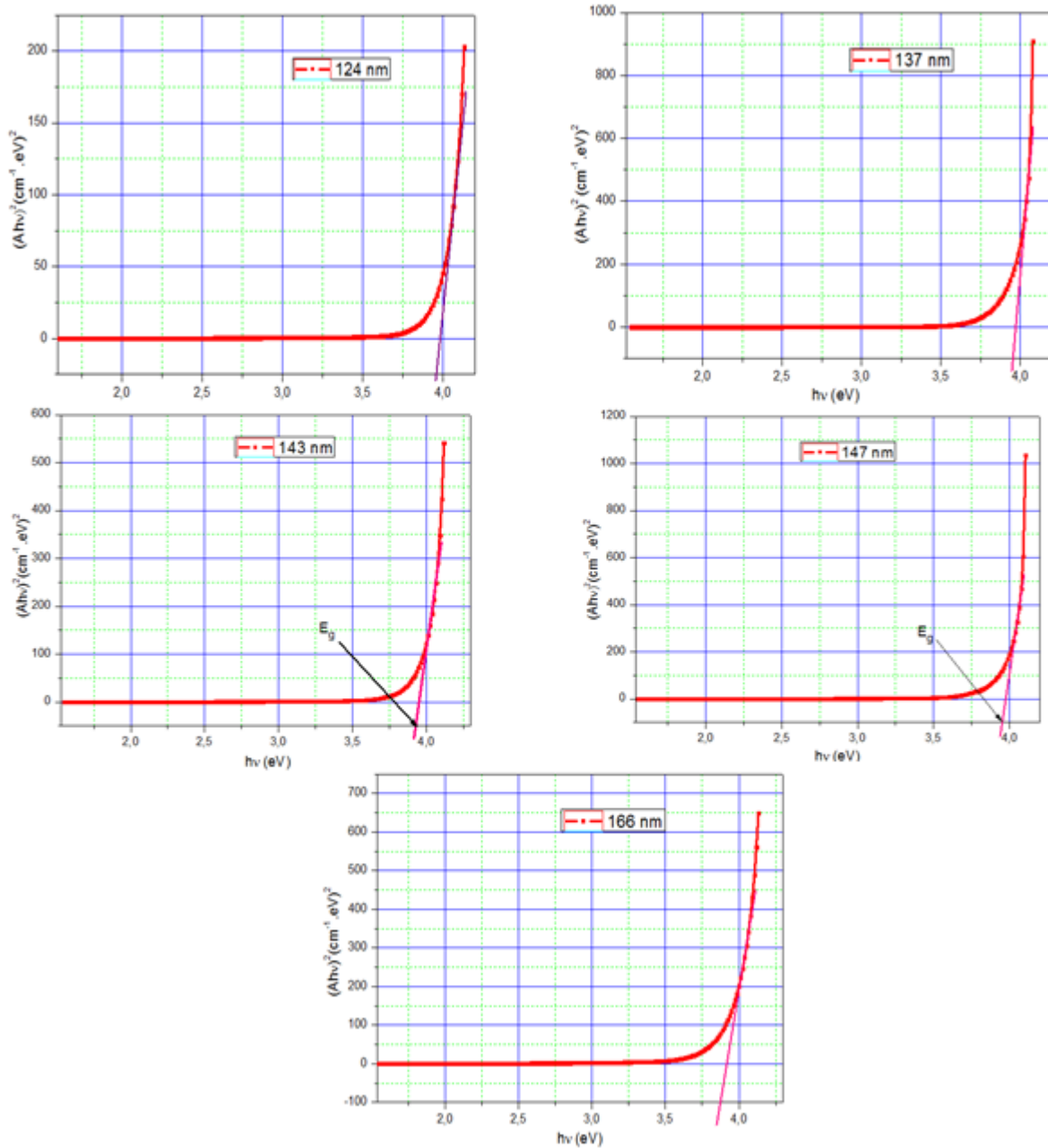
Fig. 3 - The variation of $(Ah\nu)^2$ as a function of $(h\nu)$ for each films thickness.

**Table 2 - The variation of optical gap and Urbach energy as a function of film thickness.**

Film Thickness d (nm)	124	137	143	147	166
Optical gap energy E_g (eV)	3.95	3.94	3.93	3.92	3.87
Urbach energy E_u meV	369	247.5	353	323	370

The same thing as the optical gap, the Urbach energy (E_u) is related to the disorder in the film network, as it is expressed as follows [16]:

$$A = A_0 \exp\left(\frac{h\nu}{E_u}\right) \tag{4}$$

where A_0 is a constant, $h\nu$ is the photon energy and E_u is the Urbach energy as presented in Table 2. The Fig. 4 shows the drawn of lnA as a function of photon energy, $h\nu$ to deduce the Urbach energy. We have obtained these

curves for each different film thickness. From Table 2, the Urbach energy decreases with increasing film thickness to minimum value that was located at 137 nm, then increased to maximum value at 166 nm. Some points have a change inversely between the Urbach energy and the optical band gap due to the tail width of the localized states within the optical band gap.
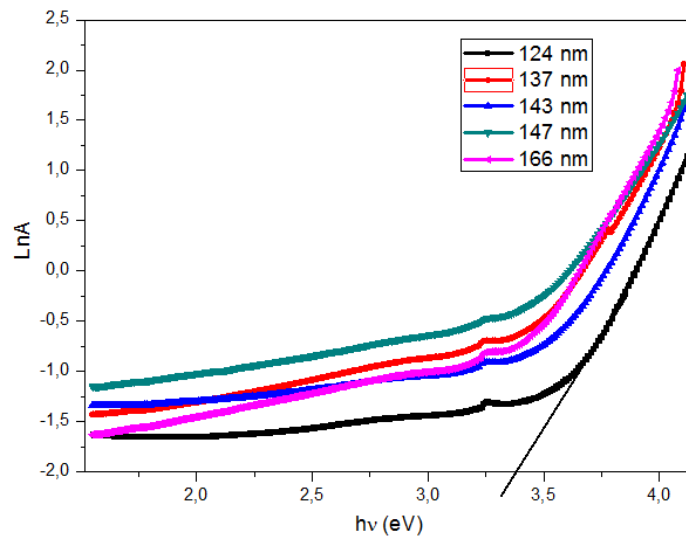

Fig. 4 - The drawn of Ln (α) as a function of *hv*.

Refractive index is an important parameter for optical materials design, and it includes valuable information for higher efficiency optical materials. Refractive index, *n* was calculated by using the following relation [17]:

$$n = \frac{1+R}{1-R} + \sqrt{\frac{4R}{(1-R)^2} - k^2}$$

(5)

where *n* is the refractive index, *R* is the reflectance and *k* is the extinction coefficient.
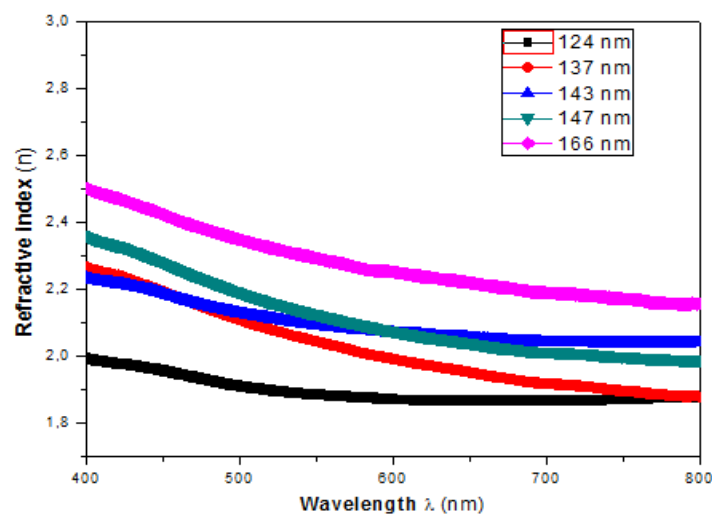
Fig. 5 - The relation between the refractive index and wavelength for Nickel Oxide thin films prepared at different film thickness.

The relation between refractive index and wavelength for spectrum range (400-800) nm of NiO thin films is shown in Fig. 5. It can be seen that the refractive index value decreases towards the longer wavelengths. This behavior reflects the typical dispersion relation in higher wavelength. The change in refractive index with the films thickness was not systematic [28]. The index of refraction is higher for shorter wavelengths of light and decreases monotonically with

increasing wavelength. However, some highly colored materials exhibit abnormal dispersion for those wavelengths of light that are strongly absorbed [17]. Results show that the refractive index values of the prepared films have values in the range of 2- 2.5 [18].

The extinction coefficient (k) was calculated using the following relation [12]:

$$k = \frac{\alpha\lambda}{4\pi} \tag{6}$$

where α is the absorption coefficient which can be estimated from the absorbance using the formula [11]:

$$\alpha = \frac{(2.303 \times A)}{t} \tag{7}$$
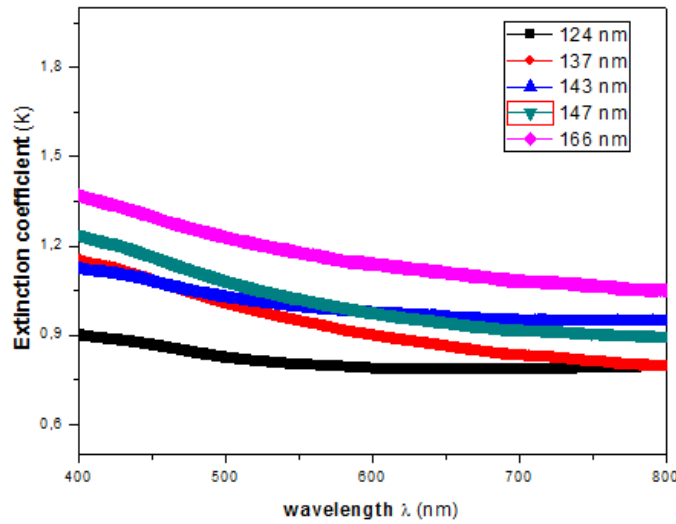
Fig. 6 - The relation between the extinction coefficient and wavelength for NiO thin films prepared at different film thickness.

The study of the extinction coefficient (k) was in the range of 400 - 800 nm, which is presented in Fig. 6. It can notice that k increases with increasing of the films thickness. The rise and fall in the value of k is directly related to the absorption of light.
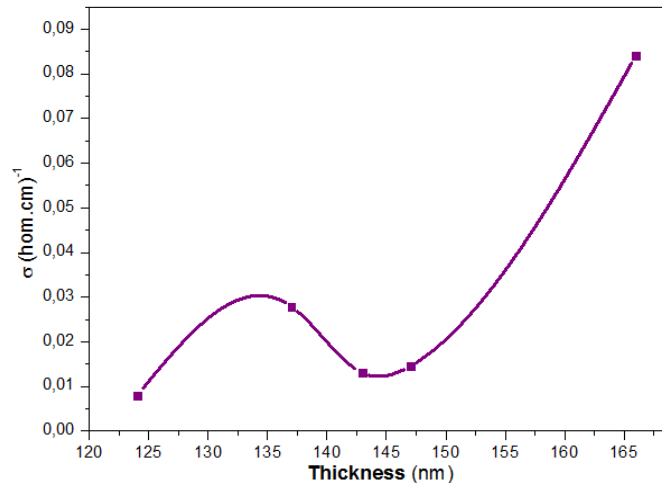
The four-point method was preferred for measurement of sheet resistance, R_{sh}. It was obtained by the following relation:

$$R_{sh} = \frac{\pi}{ln2}\frac{V}{I} \tag{8}$$

where I is the applied currant = 0,5.10-6 and V is the measurement voltage. The electrical conductivity equals to the inverse of electrical resistivity as the following equations:

$$\sigma = \frac{1}{\rho} \tag{9}$$

$$\sigma = \frac{\pi}{ln2}d\frac{V}{I} = 4.5324d\frac{V}{I} \tag{10}$$

Fig. 7 - Variation of the conductivity of NiO films as a function of film thickness.

Fig. 7 shows the variation of electrical conductivity of NiO films with different film thicknesses. As seen, the electrical conductivity firstly increased from 7.94×10^{-3} to 27.89×10^{-3} $(\Omega.cm)^{-1}$ when film thickness increases from 124 to 137 nm, then decreased to 13.37×10^{-3} $(\Omega.cm)^{-1}$ at 143 nm. It was found increased at 166 nm to maximum value of 84×10^{-3} $(\Omega.cm)^{-1}$. As a result of the compositional changes, especially the formation of nickel vacancies, this leads to p-type conductivity. The increase in the electrical conductivity variation with film thickness these results are consistent with the increase of the lattice parameter upon increasing the oxygen when we make the annealing.

4. Conclusion

In summary, NiO thin films with different thicknesses have been deposited using a sol-gel spin coating method on glass substrates. We varied the number of coatings in order to produce different thicknesses of the thin films. Structural, optical and electrical properties were investigated. The NiO thin films were observed as nanocrystalline with cubic structure at 166 nm with peaks observed at (111) and (200). All NiO thin films have an average transmittance of about 80% in the visible region. The NiO thin films have a variety in the band gap energy from 3.87 to 3.94 eV. Because of the effect of deposition times, the minimum value was found at 166 nm where this condition has the highest Urbach energy. The NiO thin films have an electrical conductivity which was increased from 7.94×10^{-3} to 84×10^{-3} $(\Omega.cm)^{-1}$ when film thickness increases from 124 to 137 nm. In the end, the electrical measurements were investigated by the four-point method, and the results shows good electrical conductivity was found at 166 nm.

5. Acknowledgement

References

[1] Verma, V., M, Katiyar. (2013). Effect of the deposition parameters on the structural and magnetic properties of pulsed laser ablated NiO thin films. Thin Solid Films, 527, 369–376.

[2] Chen, S.C., Kuo, T.Y., Lin, Y.C., Lin, H.C. (2011). Preparation and properties of p-type transparent conductive Cu-doped NiO films. Thin Solid Films, 519, 4944–4947.

[3] Sharma, R., Acharya, A.D., Shrivastava, S.B., Patidar, M.M., Gangrade, M., Shripathi, T., Ganesan, V. (2016). Studies on the structure optical and electrical properties of Zn-doped NiO thin films grown by spray pyrolysis. Optik, 127, 4661–4668.

[4] Benramache S., Aouassa, M. (2016). Preparation and Characterization of p–Type Semiconducting NiO Thin Films Deposited by Sol–Gel Technique. J. Chem. Mater. Res., 5, 119–122.

[5] Dendouga, S., Benramache, S., Lakel, S. (2016). Influence of film thickness on optical and electrical properties of Nickel Oxide (NiO) thin films. J. Chem. Mater. Res., 5, 2016, 78–84.

[6] Dini, D.,Halpin, Y., Vos, J.G., Gibson, E.A. (2015). The influence of the preparation method of NiO x photocathodes on the efficiency of p-type dye-sensitized solar cells. Coord. Chem. Rev., 304–305, 179–201.

[7] Cai, G.F., Gu, C.D., Zhang, J., Liu, P.C., Wang, X.L., You, Y.H., Tu, J.P. (2013). Ultra fast electrochromic switching of nanostructured NiO films electrodeposited from choline chloride-based ionic liquid. Electrochim. Acta, 87, 341– 347.

[8] Nwanya, A.C., Offiah, S.U., Amaechi, I.C., Agbo, S., Ezugwu, S.C., Sone, B.T., Osuji, R.U., Maaza, M., Ezema, F.I. (2015). Electrochromic and electrochemical supercapacitive properties of Room Temperature PVP capped Ni(OH)$_2$/NiO Thin Films. Electrochim. Acta, 171, 128–141.

[9] Romero, R., Martin, F., Ramos-Barrado, J.R., Leinen, D. (2010). Synthesis and characterization of nanostructured nickel oxide thin films prepared with chemical spray pyrolysis. Thin Solid Films, 518, 4499–4502.

[10] Chtouki, T., Soumahoro, L., Kulyk, B., Bougharraf, H., Kabouchi, B., Erguig, H., Sahraoui, B. (2017). Comparison of structural, morphological, linear and nonlinear optical properties of NiO thin films elaborated by Spin-Coating and Spray Pyrolysis. Optik, 128, 8–13.

[11] Yan, W., Weng, W., et al., (2008). Structures and magnetic properties of (Fe, Li)-codoped NiO thin films. Appl. Phys. Lett., 92, 052508.

[12] Chen, X., Zhao, L., Niu, Q. (2012). Electrical and Optical Properties of p-Type Li, Cu-Codoped NiO Thin Films. J. Electr. Mater., 41, 382–3386.

[13] Qureshi, A., Mergen, A., Altindal, A. (2009). Preparation and characterization of Li and Ti codoped NiO nanocomposites for gas sensors applications. Sensors and Actuators B: Chemical, 135, 537–540.

[14] Aoun, Y., Marrakchi, M., Benramache, S., Benhaoua, B., Lakel, S., Cheraf, A. (2018). Preparation and Characterizations of Monocrystalline Na Doped NiO Thin Films. Mater. Res., 21.

[15] Benramache, S., Benhaoua, B. (2012). Influence of substrate temperature and Cobalt concentration on structural and optical properties of ZnO thin films prepared by Ultrasonic spray technique. Superlattices Microstruct., 52, 807–815.

[16] Benramache, S., Benhaoua, B. (2012). Influence of annealing temperature on structural and optical properties of ZnO: In thin films prepared by ultrasonic spray technique. Superlattices Microstruct., 52, 1062–1070.

[17] Sharma, R., Acharya, A.D., Shrivastava, S.B., Shripathi, T., Ganesan, V. (2014). Preparation and characterization of transparent NiO thin films deposited by spray pyrolysis technique. Optik, 125, 6751–6756.

[18] Sajilal, K., Moses Ezhil Raj A. (2016). Effect of thickness on physico-chemical properties of p-NiO(bunsenite) thin films prepared by the chemical spray pyrolysis (CSP) technique. Optik, 127, 1442–1449.